

Supporting Information

Does Intrinsic Photocontrollable Oxidase-Mimicking Activity of 2-Aminoterephthalic Acid Dominate the Activity of Metal–Organic Framework?

Ying Nian, Linpin Luo, Wenxin Zhu, Chengyuan Yang, Liang Zhang, Min Li,
Wentao Zhang*, Jianlong Wang*

College of Food Science and Engineering, Northwest A&F University, Yangling
712100, Shaanxi, China. E-mail: wanglong79@nwsuaf.edu.cn

Equipments.

UV-visible absorption spectra were obtained using a UV-2550 UV-vis spectrophotometer (Shimadzu, Japan). The image of field emission scanning electron microscope (SEM) was taken on an S-4800 (Hitachi, Japan). Powder X-ray diffraction (XRD) patterns were recorded on a powder diffractometer (Bruker D8 Advanced Diffractometer System, Germany) with a Cu K α (1.5418 Å) source. X-ray photoelectron spectroscopy (XPS) data were recorded on a Thermo Scientific ESCALAB 250 with an Al K α source (1486.6 eV).

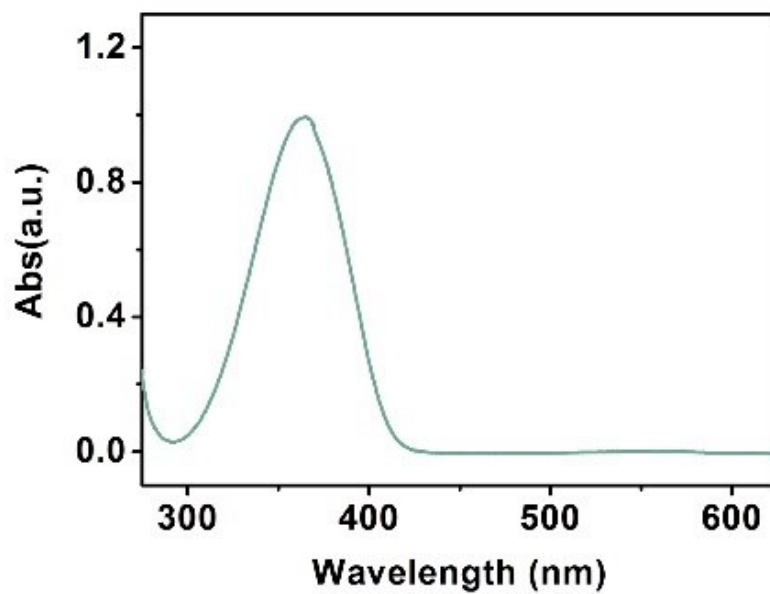


Figure S1. The UV-vis absorption spectrum of 2-Aminoterephthalic Acid (ATA).

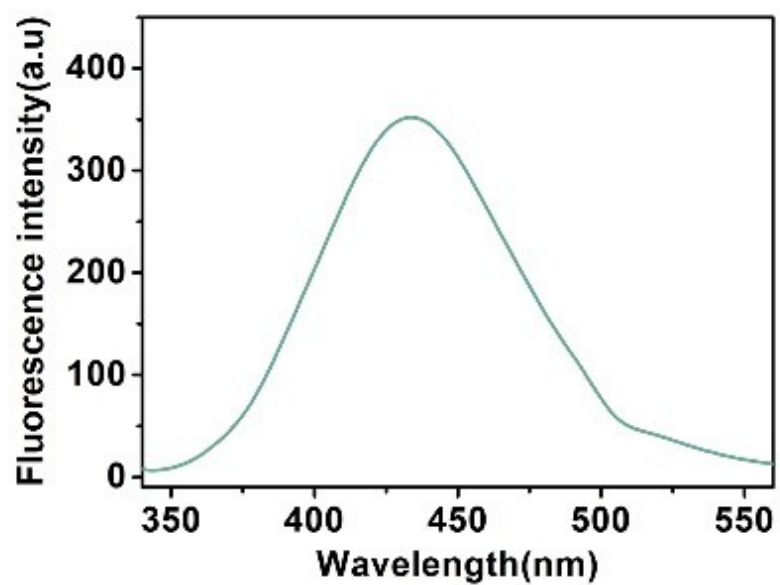


Figure S2. Photoluminescence (PL) spectrum of ATA.

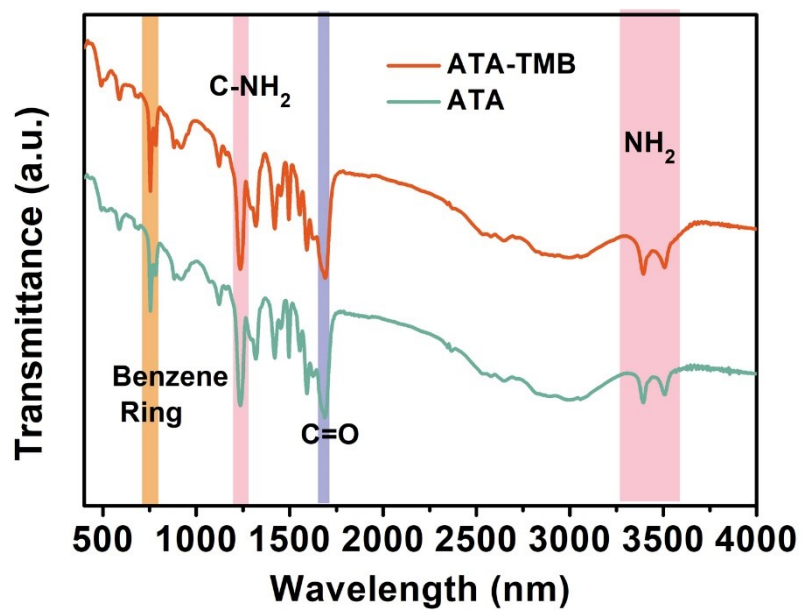


Figure S3. Fourier transform infrared spectroscopy (FTIR) spectra of ATA before and after oxidase-like catalytic reaction.

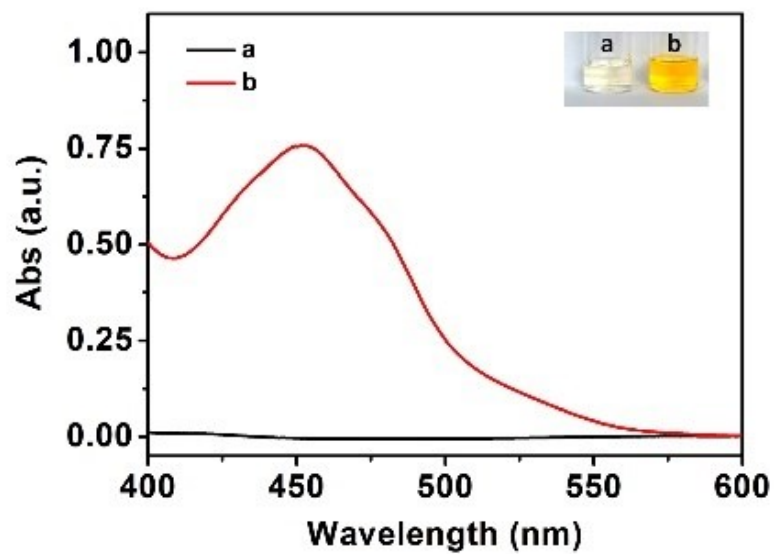


Figure S4. The UV-vis absorption spectra of different systems in acetate buffer solution (pH 3.0): a) OPD under light irradiation, b) ATA-OPD under light irradiation. Inset are the corresponding photographs.

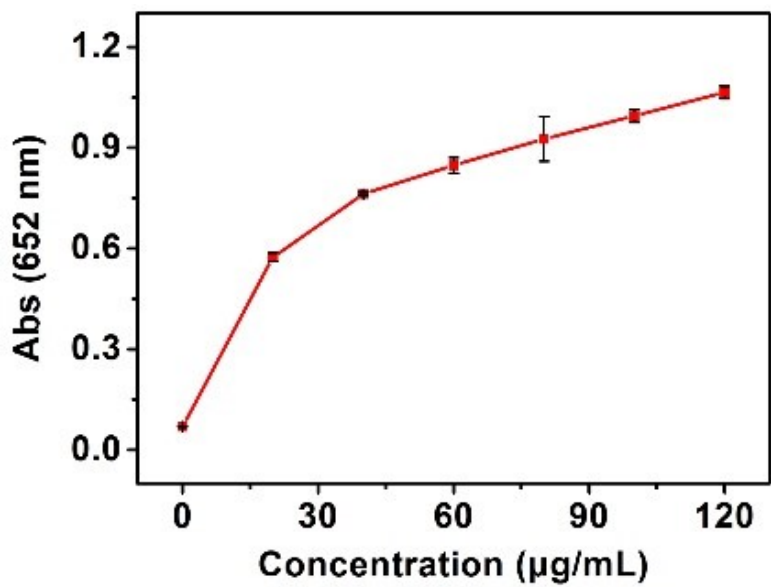


Figure S5. Relationship between catalytic activity and ATA concentration.

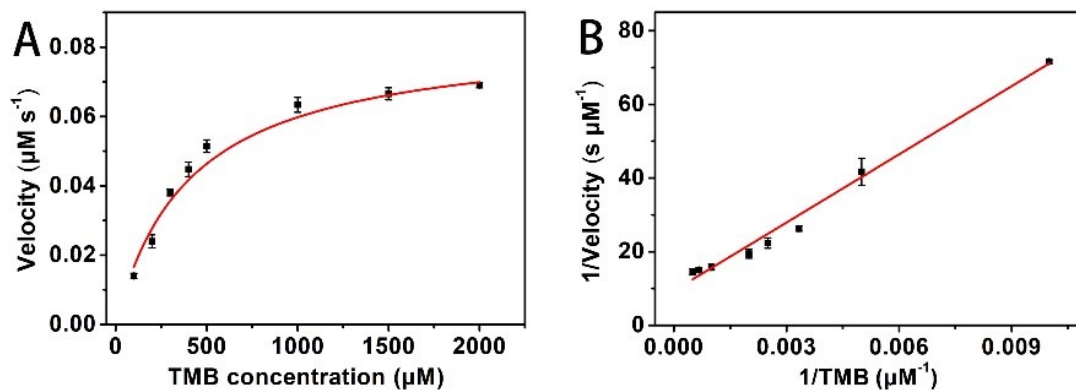


Figure S6. (A) Steady-state kinetic assays. The nonlinear fitting of Michaelis–Menten curves of ATA with TMB as substrate and (B) corresponding double-reciprocal plot.

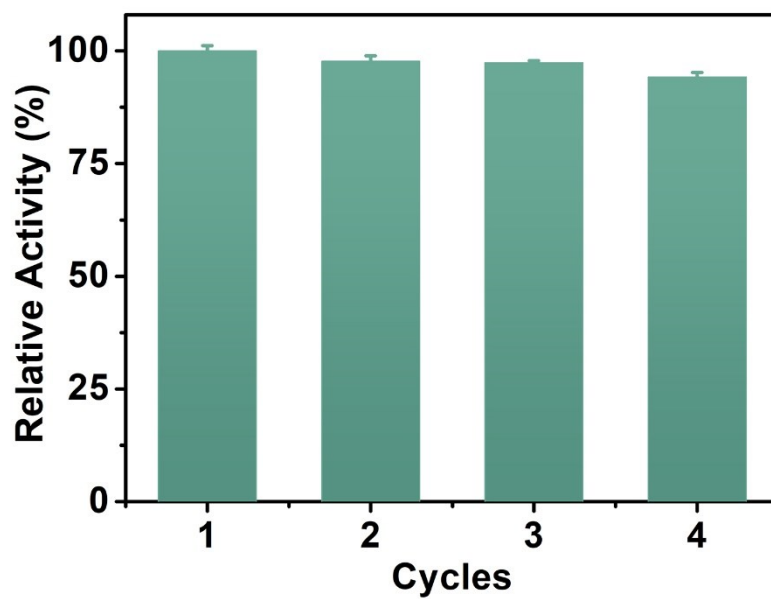


Figure S7. Photooxidase-like activity of ATA during repetitive cycles. Activity of 100% is set where absorbance is highest and the relative activities for others are calculated accordingly.

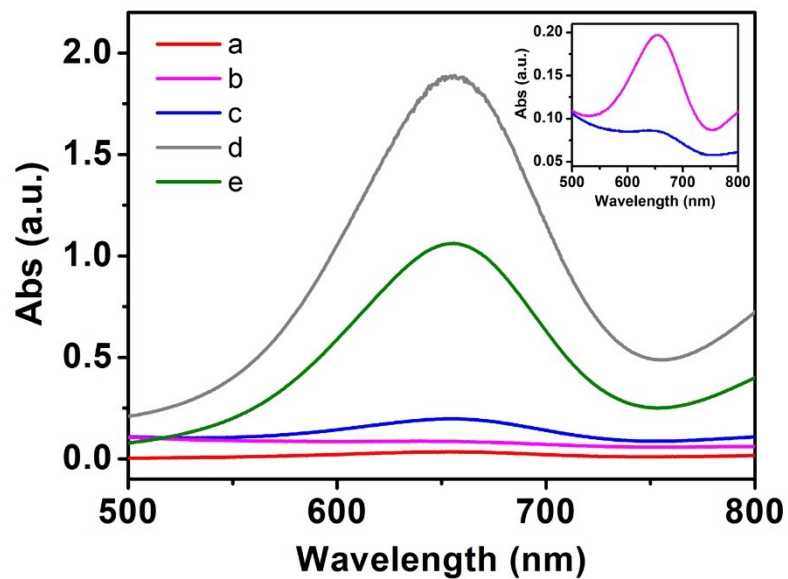


Figure S8. The UV absorption spectra of different system in acetate buffer solution (pH 3.0) with 5 min or 30 s (e)incubation (a-d): a) TMB under visible light irradiation, b) Al-MOF + TMB (no light irradiation), c) Al-MOF + TMB under UV light irradiation, d) Al-MOF + TMB under visible light irradiation, e) ATA + TMB under visble light irradiation. Inset: the closer view of b and c.

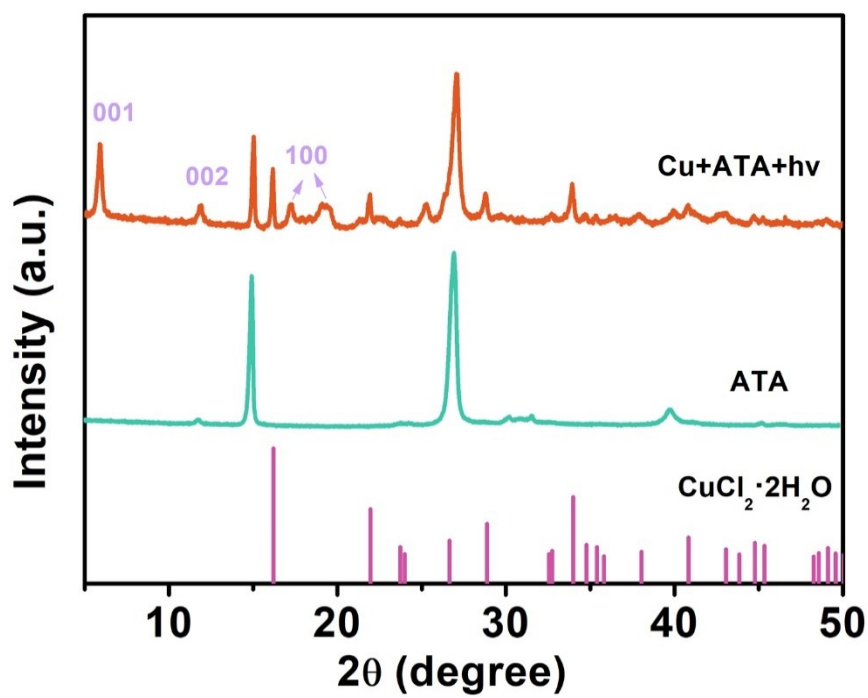


Figure S9. XRD pattern of $\text{CuCl}_2 \cdot 2\text{H}_2\text{O}$, ATA before and after incubation with $\text{Cu}(\text{II})$ under light exposure.

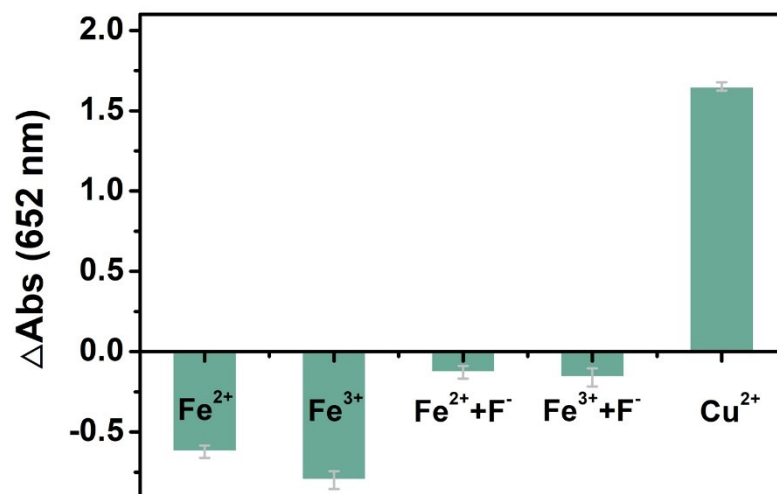


Figure S10. Selectivity test of Cu²⁺ against Fe²⁺ (50 μM) and Fe³⁺ (12.5 μM) in the absence and presence of masking agent (F⁻).

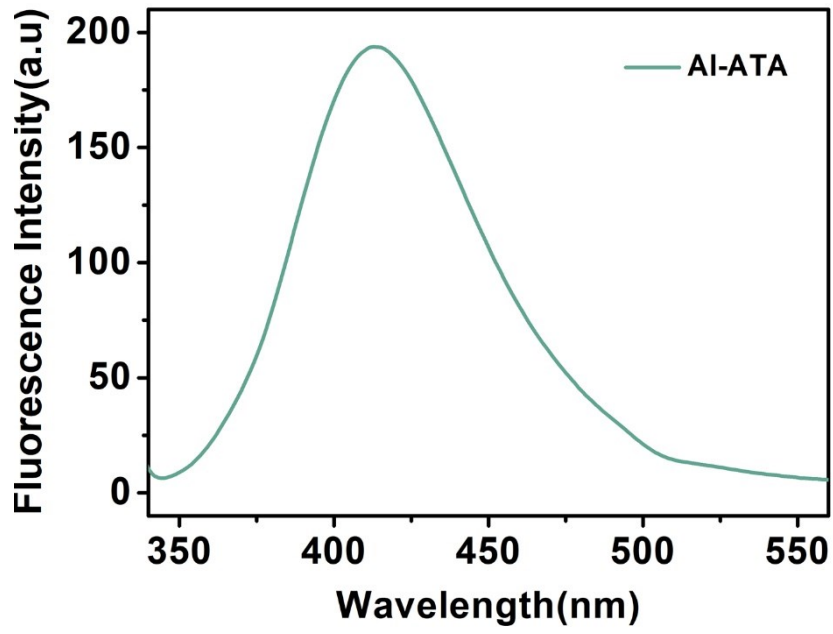


Figure S11. Fluorescence spectrum of the as-prepared Al-ATA

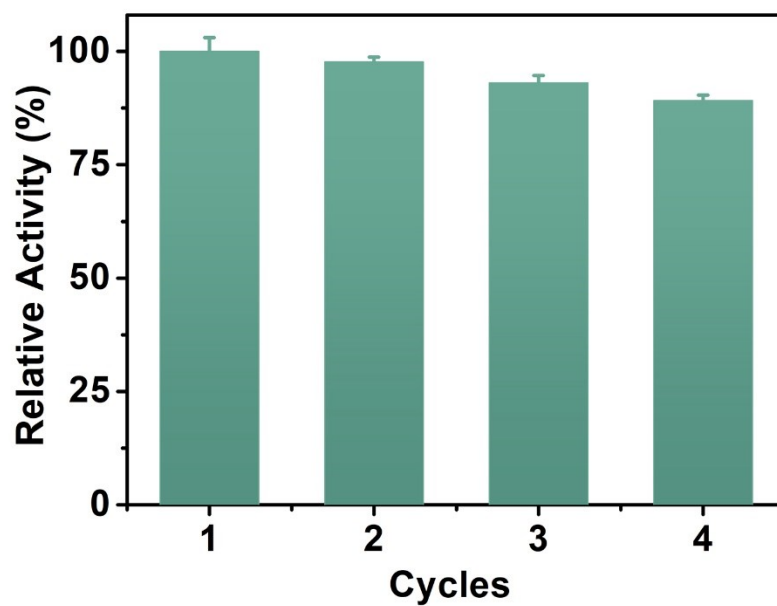


Figure S12. Photooxidase-like activity of Al-ATA during repetitive cycles. Activity of 100% is set where absorbance is highest and the relative activities for others are calculated accordingly.

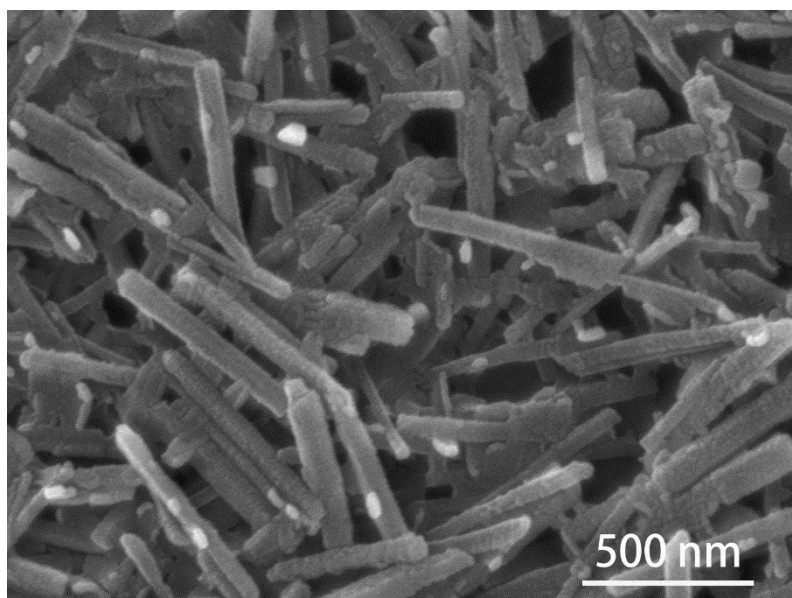


Figure S13. SEM of Al-MOF after catalytic oxidization of TMB.

Table S1 Kinetics parameters of ATA and HRP with TMB as the substrate.

Catalyst	K_m (mM)	V_{max} (10^{-8} M s $^{-1}$)	Ref.
HRP	0.434	10	1
ATA	0.407	8.41	This work

REFERENCE

1. L. Gao, J. Zhuang, L. Nie, J. Zhang, Y. Zhang, N. Gu, T. Wang, J. Feng, D. Yang, S. Perrett and X. Yan, Intrinsic Peroxidase-Like Activity of Ferromagnetic Nanoparticles, *Nat. Nanotechnol.*, 2007, **2**, 577-583.